Journal of Pure and Applied Mathematics: Advances and Applications
Volume 9, Number 1, 2013, Pages 17-41

UNSTEADY NATURAL CONVECTION BOUNDARY LAYER HEAT AND MASS TRANSFER FLOW WITH EXOTHERMIC CHEMICAL REACTIONS

KH. ABDUL MALEQUE

Professor of Mathematics
American International University-Bangladesh
House-23, 17, Kamal Ataturk Avenue
Banani, Dhaka-1213
Bangladesh
e-mail: maleque@aiub.edu
malequekh@gmail.com

Abstract

Effect of exothermic chemical reaction on an unsteady natural convection heat and mass transfer boundary layer flow past a flat porous plate is investigated. The effect of Arrhenius activation energy on the velocity, temperature, and concentration are also studied in this paper. The governing partial differential equations are reduced to ordinary differential equations by introducing locally similarity transformation (Maleque [9]). Numerical solutions to the reduced nonlinear similarity equations are then obtained by adopting Runge-Kutta and shooting methods by using the Nachtsheim and Swigert iteration technique. The results of the numerical solution are then presented graphically in the form of velocity, temperature, and concentration profiles. The corresponding skin friction coefficient, the Nusselt number, and the Sherwood number are also calculated and displayed in a table showing the effects of various parameters on them.

2010 Mathematics Subject Classification: 76-XX.

Keywords and phrases: exothermic reactions, heat and mass transfer, activation energy, porous plate.

Received September 25, 2012; Revised October 20, 2012

Nomenclature

(u, v) : Components of velocity field.

N_u : Nusselt number.

T : Temperature of the flow field.

T_w : Temperature at the plate.

E_a : The activation energy.

S_c : Schmidt number.

G_r : Grashof number.

c_p : Specific heat at constant pressure.

P_r : Prandtl number.

S_h : Sherwood number.

T_∞ : Temperature of the fluid at infinity.

f : Dimensionless similarity functions.

k : The Boltzmann constant.

E : The non-dimensional activation energy.

G_m : Modified (Solutal) Grashof number.

Greek symbols

θ : Dimensionless temperature.

η : Dimensionless similarity variable.

ν : Kinematic viscosity.

κ : Thermal conductivity.

μ : Fluid viscosity.

ϕ : Dimensionless concentration.

δ : Scale factor.

ρ : Density of the fluid.

τ : Shear stress.

λ^2 : The non-dimensional chemical reaction rate constant.

β and β^* : The coefficients of volume expansions for temperature and concentration, respectively.

1. Introduction

An exothermic reaction is a chemical reaction that releases energy in the form of light and heat. It gives out energy to its surroundings. The energy needed for the reaction to occur is less than the total energy released. Energy is obtained from chemical bonds. When bonds are broken, energy is required. When bonds are formed, energy is released. Each type of bond has specific bond energy. It can be predicted whether a chemical reaction will release or require heat by using bond energies. When there is more energy used to form the bonds than to break the bonds, heat is given out. This is known as an exothermic reaction. When a reaction requires an input of energy, it is known as an exothermic reaction. Activation energy is the ability to break bonds. In free convection boundary layer flows with simultaneous heat mass transfer, one important criteria that is generally not encountered is the species chemical reactions with finite Arrhenius activation energy. The Arrhenius law is usually of the form (Tencer et al. [16])

$$K = B \exp\left[\frac{-E_a}{k(T - T_\infty)}\right], \tag{1}$$

where K is the rate constant of chemical reaction and B is the pre-exponential factor simply prefactor (constant), is based on the fact that increasing the temperature frequently causes a marked increase in the rate of reactions. E_a is the activation energy and $k = 8.61 \times 10^{-5}\text{eV/K}$ is the Boltzmann constant, which is the physical constant relating energy at the individual particle level with temperature observed at the collective or bulk level. It is the gas constant R divided by the Avogadro constant N_A

$$k = \frac{R}{N_A}. \tag{2}$$

In areas such as geothermal or oil reservoir engineering, the above phenomenon is usually applicable. Apart from experimental works in these areas, it is also important to make some theoretical efforts to predict the effects of the activation energy in flows mentioned above. But in this regard, very few theoretical works are available in literature. The reason is that, the chemical reaction processes involved in the system are quite complex and generally the mass transfer equation that is required for all the reactions involved also become complex. Theoretically, such an equation is rather impossible to tackle. From chemical kinetic viewpoint, this is a very difficult problem, but if the reaction is restricted to binary type, a lot of progress can be made. The thermo-mechanical balance equations for a mixture of general materials were first formulated by Truesdell [17]. Thereafter, Mills [10] and Beevers and Craine [3] have obtained some exact solutions for the boundary layer flow of a binary mixture of incompressible Newtonian fluids. Several problems relating to the mechanics of oil and water emulsions, particularly with regard to applications in lubrication practice, have been considered within the context of a binary mixture theory by Al-Sharif et al. [2] and Wang et al. [18].

A simple model involving binary reaction was studied by Bestman [4]. He considered the motion through the plate to be large, which enabled him to obtain analytical solutions (subject to same restrictions) for

various values of activation energy by employing the perturbation technique proposed by Singh and Dikshit [14]. Bestman [5] and Alabraba et al. [1] took into account the effect of the Arrhenius activation energy under the different physical conditions. Convection instabilities induced exothermic reactions occurring in a porous medium was investigated by Subramanian and Balakotaiah [15].

Kandasamy et al. [6] studied the combined effects of chemical reaction, heat and mass transfer along a wedge with heat source and concentration in the presence of suction or injection. Their result shows that the flow field is influenced appreciably by chemical reaction, heat source, and suction or injection at the wall of the wedge. Recently, Makinde et al. [7] studied the problems of unsteady convection with chemical reaction and radiative heat transfer past a flat porous plate moving through a binary mixture in an optically thin environment. More recently, Pochai and Jaisaardsuetrong [12] presented a numerical solution of an exothermic reactions model with constant heat source in a porous medium by using finite difference method. In the present paper, we investigate a numerical solution of an unsteady natural convection heat and mass transfer boundary layer flow past a flat porous plate taking into account the effects of Arrhenius activation energy and exothermic chemical reaction.

2. Governing Equations

We consider the boundary wall to be of infinite extend so that all quantities are homogeneous in x and hence all derivatives with respect to x are neglected. Thus, the governing equations are

$$\frac{\partial \nu}{\partial y} = 0, \tag{3}$$

$$\frac{\partial u}{\partial t} + \nu \frac{\partial u}{\partial y} = \upsilon \frac{\partial^2 u}{\partial y^2} + g\beta(T - T_\infty) + g\beta^*(C - C_\infty), \tag{4}$$

$$\rho c_p\left(\frac{\partial T}{\partial t}+\nu\frac{\partial T}{\partial y}\right)=\kappa\frac{\partial^2 T}{\partial y^2}+k_r^2(T-T_\infty)^w\exp\left[\frac{-E_a}{k(T-T_\infty)}\right](C-C_\infty), \quad (5)$$

$$\frac{\partial C}{\partial t}+\nu\frac{\partial C}{\partial y}=D_m\frac{\partial^2 C}{\partial y^2}-k_r^2(T-T_\infty)^w\exp\left[\frac{-E_a}{k(T-T_\infty)}\right](C-C_\infty). \quad (6)$$

The boundary conditions of above system are

$$\left.\begin{aligned} &u=U_0,\ \nu=\nu(t),\ T=T_w,\ C=C_w \ \text{ at } \ y=0,\\ &u=0,\ T\to T_\infty,\ C\to C_\infty \quad \text{at } \ y=\infty. \end{aligned}\right\}, \quad (7)$$

where (u, ν) is the velocity vector, U_0 is the plate velocity, T is the temperature, C is the concentration of the fluid, v is the kinemetic coefficient of viscosity, β and β^* are the coefficients of volume expansions for temperature and concentration, respectively, κ is the heat diffusivity coefficient, c_p is the specific heat at constant pressure, D_m is the coefficient of mass diffusivity, k_r^2 is the exothermic chemical reaction rate constant, and $(T-T_\infty)^w\exp\left[\frac{-E_a}{k(T-T_\infty)}\right]$ is the Arrhenius function, where w is a unit less constant exponent fitted rate constants typically lie in the range $-1 < w < 1$.

(http://www.iupac.org/goldbook/mo3963.pdf)

3. Mathematical Formulations

In order to solve the governing equations (3) to (6) under the boundary conditions (7), we adopt the well defined similarity technique to obtain the similarity solutions. For this purpose, the following non-dimensional variables are now introduced:

$$\eta=\frac{y}{\delta(t)}, \quad \frac{u}{U_0}=f(\eta), \quad \frac{T-T_\infty}{T_w-T_\infty}=\theta(\eta), \quad \text{and} \quad \frac{C-C_\infty}{C_w-C_\infty}=\phi(\eta). \quad (8)$$

From the equation of continuity (3), we have

$$\nu(t) = -\frac{\nu_0 v}{\delta(t)}, \tag{9}$$

where ν_0 is the dimensionless suction or injection velocity at the plate, $\nu_0 > 0$ corresponds to suction and $\nu_0 < 0$ corresponds to injection.

Introducing the dimensionless quantities from Equation (8) and ν from Equation (9) in Equations (4), (5), and (6), we finally obtain the nonlinear ordinary differential equations as

$$f'' + \eta \frac{\delta\delta'}{v} f' + \nu_0 f' + G_r\theta + G_m\phi = 0, \tag{10}$$

$$P_r^{-1}\theta'' + (\eta \frac{\delta\delta'}{v} + \nu_0)\theta' + \lambda^2 \exp(-\frac{E}{\theta})\theta^w\phi = 0, \tag{11}$$

$$S_c^{-1}\phi'' + (\eta \frac{\delta\delta'}{v} + \nu_0)\phi' - \lambda^2 \exp(-\frac{E}{\theta})\theta^w\phi = 0. \tag{12}$$

Here, Grashof number $G_r = \frac{g\beta(T_w - T_\infty)\delta^2}{vU_0}$, modified (Solutal) Grashof number $G_m = \frac{g\beta^*(C_w - C_\infty)\delta^2}{vU_0}$, Prandtl number $P_r = \frac{\rho v c_p}{\kappa}$, the chemical reaction rate constant $\lambda^2 = \frac{k_r^2\delta^2(T_w - T_\infty)^w}{v}$, Schmidt number $S_c = \frac{v}{D_M}$, the non-dimensional activation energy $E = \frac{E_a}{k(T_w - T_\infty)}$.

The Equations (10) to (12) are similar except for the term $\frac{\delta\delta'}{v}$, where time t appears explicitly. Thus, the similarity condition requires that $\frac{\delta\delta'}{v}$ must be a constant quantity. Hence following Maleque [9], one can try a class of solutions of the Equations (10) to (12) by assuming that

$$\frac{\delta\delta'}{v} = A \text{ (constant)}. \tag{13}$$

From Equation (11), we have

$$\delta(t) = \sqrt{2Avt} + L, \tag{14}$$

where the constant of integration L is determined through the condition that $\delta = L$ when $t = 0$. Here $A = 0$ implies that $\delta = L$ represents the length scale for steady flow and $A \neq 0$, that is, δ represents the length scale for unsteady flow. Let us now consider a class of solutions for which $A = 2$ and hence the length scale δ from Equation (12) becomes

$$\delta(t) = 2\sqrt{vt} + L, \tag{15}$$

which exactly corresponds to the usual scalling factor considered for various unsteady boundary layer flow Schlichting [13]. Since δ is a scaling factor as well as similarity parameter, any other values of A in Equation (14) would not be change the nature of the solution except that the scale would be different. Finally, introducing Equation (15) in Equations (10) to (12), respectively, we have the following dimensionless nonlinear ordinary differential equations:

$$f'' + (2\eta + \nu_0)f' + G_r\theta + G_m\phi = 0, \tag{16}$$

$$P_r^{-1}\theta'' + (2\eta + \nu_0)\theta' + \lambda^2 \exp\left(-\frac{E}{\theta}\right)\theta^w\phi = 0, \tag{17}$$

$$S_c^{-1}\phi'' + (2\eta + \nu_0)\phi' - \lambda^2 \exp\left(-\frac{E}{\theta}\right)\theta^w\phi = 0. \tag{18}$$

The boundary conditions equation (4) then becomes

$$\left.\begin{aligned} f(0) = 1, \quad \theta(0) = 1, \quad \phi(0) = 1 \\ f(\infty) = 0, \quad \theta(\infty) = 0, \quad \phi(\infty) = 0 \end{aligned}\right\}. \tag{19}$$

In all over equations, primes denote the differentiation with respect to η. Equations (16) to (18) are solved numerically under the boundary conditions (19) by using Nachtsheim and Swigert iteration technique.

4. Numerical Solutions

Equations (16)-(18) are solved numerically under the boundary conditions (19) by using Nachtsheim and Swigert [11] iteration technique. In Equation (19), there are three asymptotic boundary conditions and hence follows three unknown surface conditions $f''(0)$, $\theta'(0)$, and $\phi'(0)$. Within the context of the initial-value method and the Nachtsheim and Swigert iteration technique, the outer boundary conditions may be functionally represented by the first order Taylor's series as

$$f(\eta_{\max}) = f(X, Y, Z) = f_c(\eta_{\max}) + \Delta X\, f_X + \Delta Y\, f_Y + \Delta Z\, f_Z = \delta_1, \quad (20)$$

$$\theta(\eta_{\max}) = \theta(X, Y, Z) = \theta_c(\eta_{\max}) + \Delta X\, \theta_X + \Delta Y\, \theta_Y + \Delta Z\, \theta_Z = \delta_2, \quad (21)$$

$$\phi(\eta_{\max}) = \phi(X, Y, Z) = \phi_c(\eta_{\max}) + \Delta X\, \phi_X + \Delta Y\, \phi_Y + \Delta Z\, \phi_Z = \delta_3, \quad (22)$$

with the asymptotic convergence criteria given by

$$f'(\eta_{\max}) = f'(X, Y, Z) = f'_c(\eta_{\max}) + \Delta X\, f'_X + \Delta Y\, f'_Y + \Delta Z\, f'_Z = \delta_4, \quad (23)$$

$$\theta'(\eta_{\max}) = \theta'(X, Y, Z) = \theta'_c(\eta_{\max}) + \Delta X\, \theta'_X + \Delta Y\, \theta'_Y + \Delta Z\, \theta'_Z = \delta_5, \quad (24)$$

$$\phi'(\eta_{\max}) = \phi'(X, Y, Z) = \phi'_c(\eta_{\max}) + \Delta X\, \phi'_X + \Delta Y\, \phi'_Y + \Delta Z\, \phi'_Z = \delta_6, \quad (25)$$

where $X = f''(0)$, $Y = \theta'(0)$, $Z = \phi'(0)$, and X, Y, Z subscripts indicate partial differentiation, e.g., $f'_Y = \dfrac{\partial f'(\eta_{\max})}{\partial \theta'(0)}$. The subscript c indicates the value of the function at $\eta_{\max}$ to be determined from the trial integration.

Solutions of these equations in a least square sense requires determining the minimum value of $E = \delta_1^2 + \delta_2^2 + \delta_3^2 + \delta_4^2 + \delta_5^2 + \delta_6^2$ with respect to $X, Y,$ and Z. To solve $\Delta X, \Delta Y,$ and ΔZ, we require to differentiate E with respect to $X, Y,$ and Z, respectively. Thus, adopting this numerical technique, a computer program was set up for the solutions of the basic nonlinear differential equations of our problem, where the integration technique was adopted as the six ordered Runge-

Kutta method of integration. The results of this integration are then displayed graphically in the form of velocity, temperature, and concentration profiles in Figures 1-11. In the process of integration, the local skin-friction coefficient, the local rates of heat and mass transfer to the surface, which are of chief physical interest are also calculated out. The equation defining the wall skin-friction is

$$\tau = -\mu\left(\frac{\partial u}{\partial y}\right)_{y=0}.$$

Hence, the skin-friction coefficient is given by

$$C_f = \frac{\tau}{\rho U_0^2}\alpha - f'(0). \tag{26}$$

The heat flux (q_w) and the mass flux (M_w) at the wall are given by

$$q_w = -\kappa\left(\frac{\partial T}{\partial y}\right)_{y=0} \quad \text{and} \quad M_w = -D_M\left(\frac{\partial C}{\partial y}\right)_{y=0}.$$

Hence, the Nusselt number (N_u) and the Sherwood number (S_h) are obtained as

$$N_u\alpha - \theta'(0), \tag{27}$$

and

$$S_h\alpha - \phi'(0). \tag{28}$$

These above coefficients are then obtained from the procedure of the numerical computations and are sorted in Table 1.

In all the computations, the step size $\Delta\eta = 0.01$ was selected that satisfied a convergence criterion of 10^{-6} in almost all of different phases mentioned above. Stating $\eta_\infty = \eta_\infty + \Delta\eta$, the value of η_∞ was found to each iteration loop $(\eta_\infty)_{\max}$, to each group of the parameters, has been obtained when value of unknown boundary conditions at $\eta = 0$ not

change to successful loop with error less than 10^{-6}. However, different step sizes such as $\Delta\eta = 0.01$, $\Delta\eta = 0.005$, and $\Delta\eta = 0.001$ were also tried and the obtained solutions have been found to be independent of the step sizes observed in Figure 12.

5. Result and Discussions

The parameters entering into the fluid flow are Grashof number G_r, Solutal (modified) Grashof number G_m, suction parameter ν_0, Prandtl number P_r, the non-dimensional exothermic chemical reaction rate constant λ^2, Schmidt number S_c, and the non-dimensional activation energy E.

It is, therefore, pertinent to inquire the effects of variation of each of them when the others are kept constant. The numerical results are thus presented in the form of velocity profiles, temperature profiles, and concentration profiles in Figures 1-11 for the different values of G_r, G_m, λ, E, and ν_0. The value of G_r is taken to be both positive and negative, since these values represent, respectively, cooling and heating of the plate.

The values of G_r is taken to be large $(G_r = 10)$, since the value corresponds to a cooling problem that is generally encountered in nuclear engineering in connection with the cooling of reactors. In air $(P_r = 0.71)$, the diluting chemical species of most common interest have Schmidt number in the range from 0.6 to 0.75. Therefore, the Schmidt number $S_c = 0.6$ is considered. In particulars, 0.6 corresponds to water vapour that represents a diffusing chemical species of most common interest in air. The values of the suction parameter ν_0 are taken to be large. Apart from the above figures and table, the representative velocity, temperature, and concentration profiles and the values of the physically important parameters, i.e., the local shear stress, the local rates of heat

and mass transfers, are illustrated for uniform wall temperature and species concentration in Figures 1-11 and in Table 1.

5.1. Effects of G_r and G_m on the velocity profiles

The velocity profiles generated due to impulsive motion of the plate is plotted in Figure 1 for both cooling $(G_r > 0)$ and heating $(G_r < 0)$ of the plate keeping other parameters fixed $(G_m = 1.0, P_r = 0.71, S_c = 0.6, \lambda = 5, \nu_0 = 3.0, E = 1.0,$ and $w = 1)$. In Figure 1, velocity profiles are shown for different values of G_r. We observe that velocity increases with increasing values of G_r for the cooling of the plate. From this figure, it is also observed that the negative increase in the Grashof number leads to the decrease in the velocity field. That is for heating of the plate (Figure 1), the effects of the Grashof number G_r on the velocity field have also opposite effects, as compared to the cooling of the plate. Solutal Grashof number $G_m > 0$ corresponds that the chemical species concentration in the free stream region is less than the concentration at the boundary surface. Figure 2 presents the effects of Solutal Grashof number G_m on the velocity profiles. It is observed that the velocity profile increases with the increasing values of Solutal Grashof number G_m.

For $G_m = 1.0$, $P_r = 0.71$, $S_c = 0.6$, $\lambda = 5$, $\nu_0 = 3.0$, $E = 1.0$, and $w = 1$.

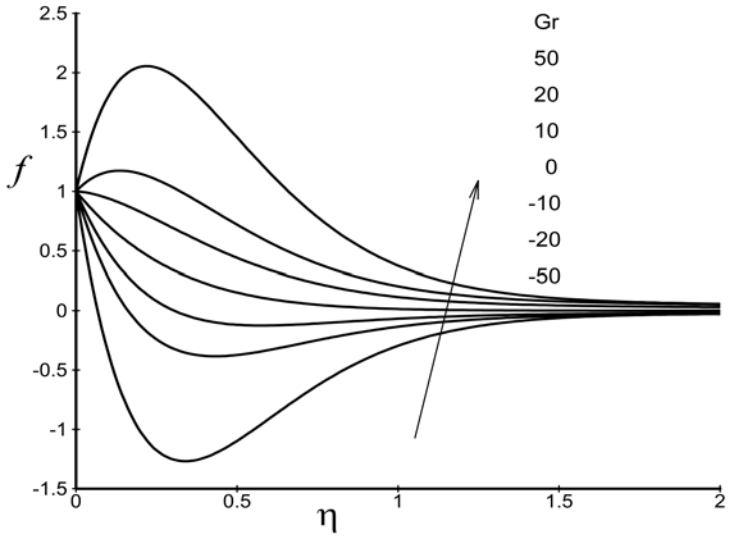

Figure 1. Effect of G_r on the velocity profiles.

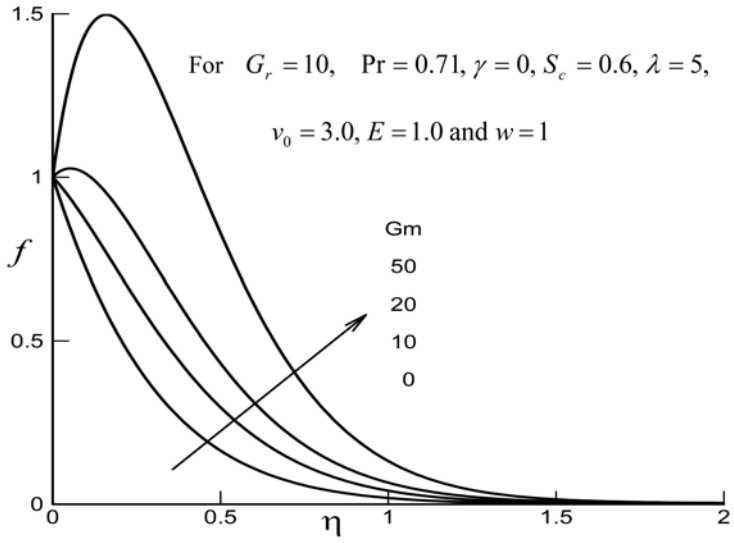

Figure 2. Effect of G_m on the velocity profiles.

5.2. Effects of λ on the concentration, the temperature, and the velocity profiles

Considering chemical reaction rate constant λ^2 is always positive. Figures 3-5 represent the effect of chemical rate constant λ on the concentration, the temperature, and the velocity profiles, respectively.

We observe from the last part of Equation (18) that $\lambda^2 \exp(-E/\theta)$ increases with the increasing values of λ. We also observe from this equation that increase in $\lambda^2 \exp(-E/\theta)$ means increase in λ leads to the decrease in the concentration profiles. This is in great agreement with Figure 3. It is observed from the Equation (1) that increasing temperature frequently causes a marked increase in the rate of reactions is shown in Figure 4. The parameter λ does not enter directly into the momentum equation, but its influence comes through the mass equation. Figure 5 shows the variation of the velocity profiles for different values of λ. The velocity profile increases with the increasing values of λ.

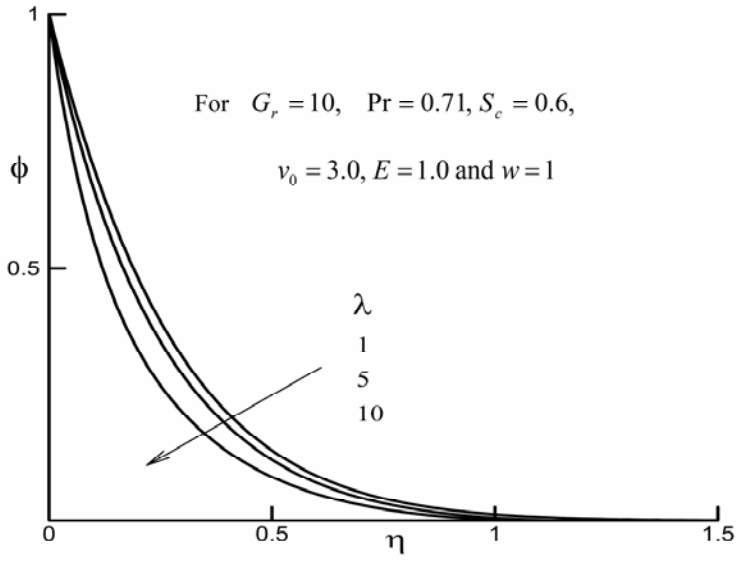

Figure 3. Effects of λ on the concentration profiles.

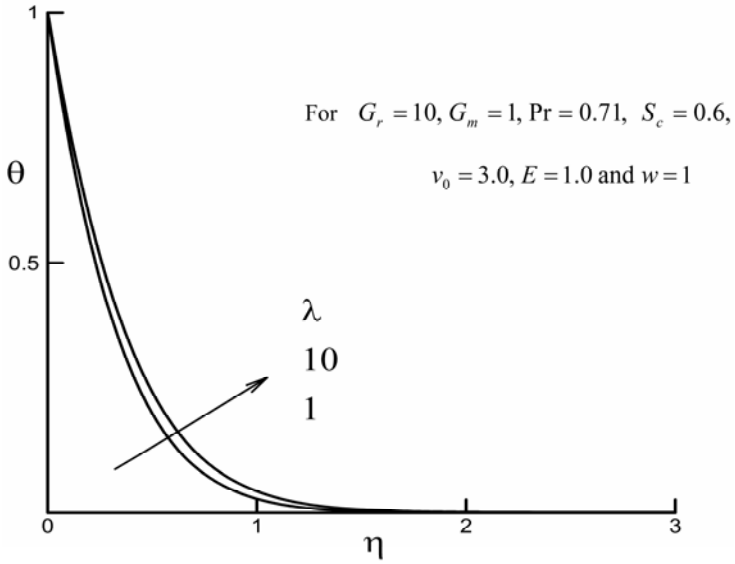

Figure 4. Effects of λ on the temperature profiles.

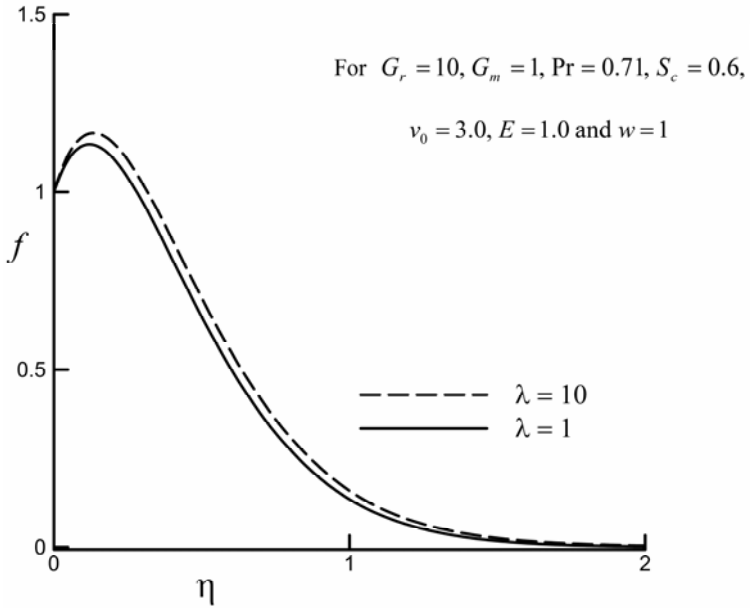

Figure 5. Effects of λ on the velocity profiles.

5.3. Effects of activation energy (E) on the concentration, the temperature, and the velocity profiles

In chemistry, Activation Energy is a term introduced in 1889 by the Swedish scientist Svante Arrhenius that is defined as the energy that must be overcome in order for a chemical reaction to occur. Activation energy may also be defined as the minimum energy required starting a chemical reaction. The activation energy of a reaction is usually denoted by E_a, and given in units of kilojoules per mole.

Activation energy can be thought of as the height of the potential barrier (sometimes called the energy barrier) separating two minima of potential energy (of the reactants and products of a reaction). For a chemical reaction to proceed at a reasonable rate, there should exist an appreciable number of molecules with energy equal to or greater than the activation energy. Effects of activation energy (E) on the concentration, the temperature, and velocity profiles are shown in Figures 6 to 8, respectively. From Equation (1), we observe that chemical reaction rate (K) decreases with the increasing values of activation energy (E_a). We also observe from Equation (18) that increase in activation energy (E) leads to decrease $\lambda^2 \exp(-E/\theta)$ as well as to increase the concentration profiles shown in Figure 6. Equation (1) suggests that the activation energy is dependent on temperature. For fixed value of chemical reaction rate constant, the temperature profile increases with the increasing values of activation energy shown in Figure 7. The parameter E does not enter directly into the momentum equation, but its influence comes through the mass equation. Figure 8 shows the variation of the velocity profiles for different values of E. From this figure, it has been observed that the velocity profile increases with the increasing values of E.

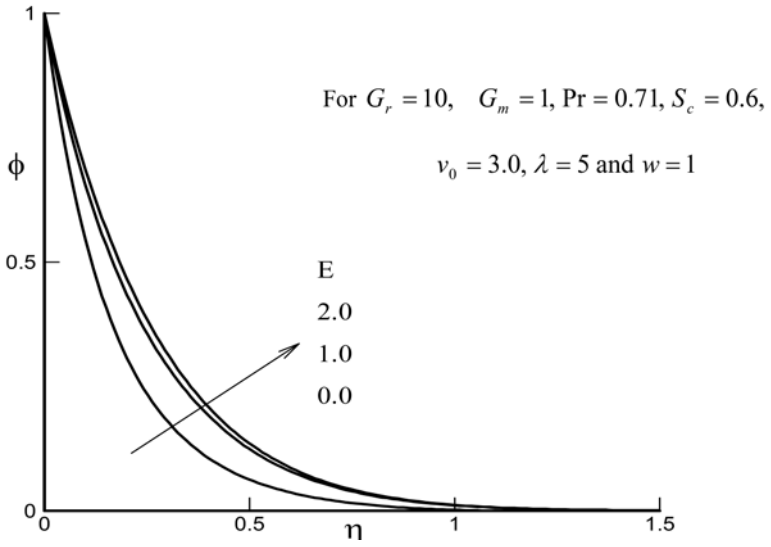

Figure 6. Effects of E on the concentration profiles.

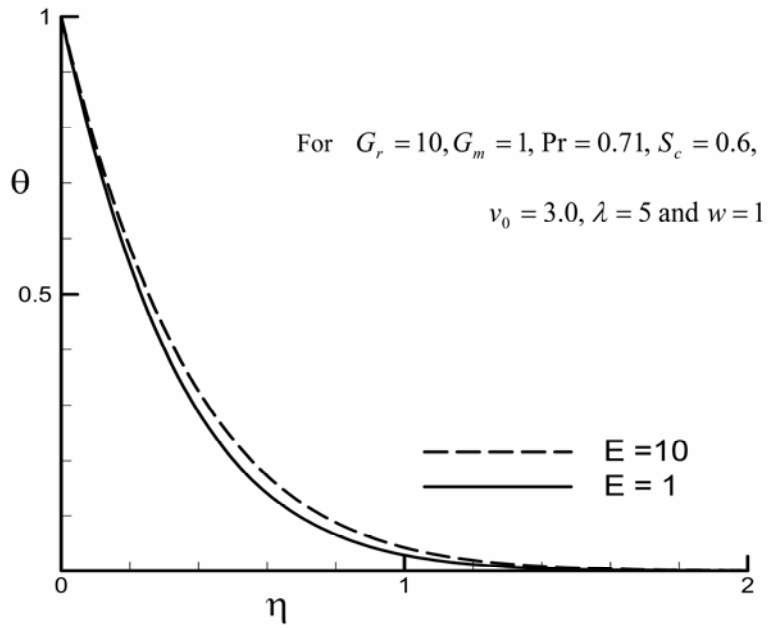

Figure 7. Effects of E on the temperature profiles.

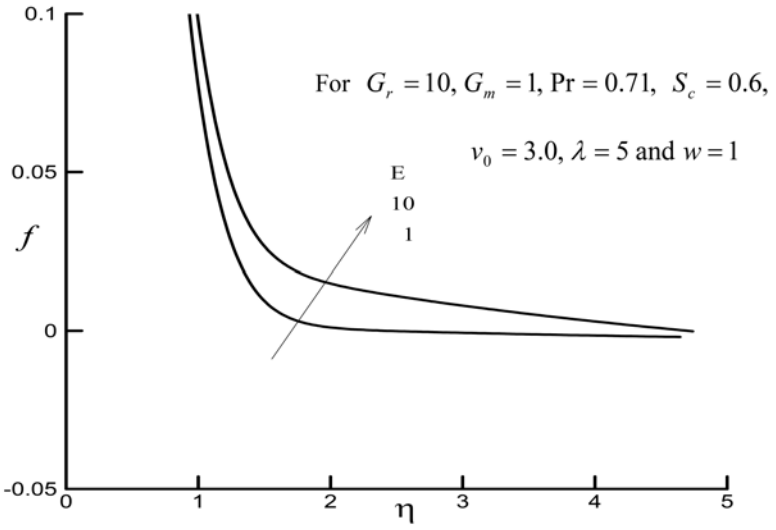

Figure 8. Effects of E on the velocity profiles.

5.4. Effects of suction/injection (ν_0) on the velocity, the temperature, and the concentration profiles

The effects of suction and injection (ν_0) for $\lambda = 5$, $E = 1$, $G_r = 5$, $G_m = 1$, $S_c = 0.6$, and $P_r = 0.7$ on the velocity profiles, temperature profiles, and concentration profiles are shown, respectively, in Figures 9 to 11. For strong suction $(\nu_0 > 0)$, the velocity, the temperature, and the concentration profiles decay rapidly away from the surface. The fact that suction stabilizes the boundary layer is also apparent from these figures. As for the injection $(\nu_0 < 0)$, from Figures 9 to 11, it is observed that the boundary layer is increasingly blown away from the plate to form an interlayer between the injection and the outer flow regions.

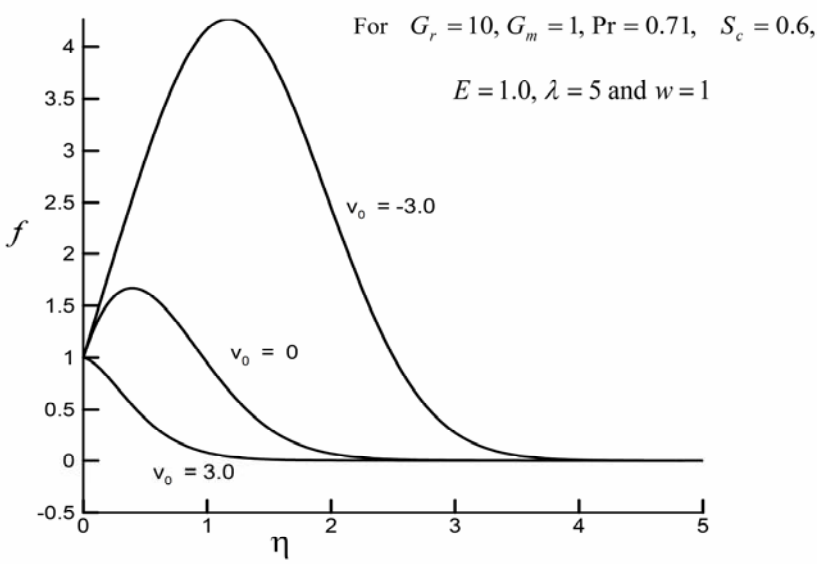

Figure 9. Effects of ν_0 on the velocity profiles.

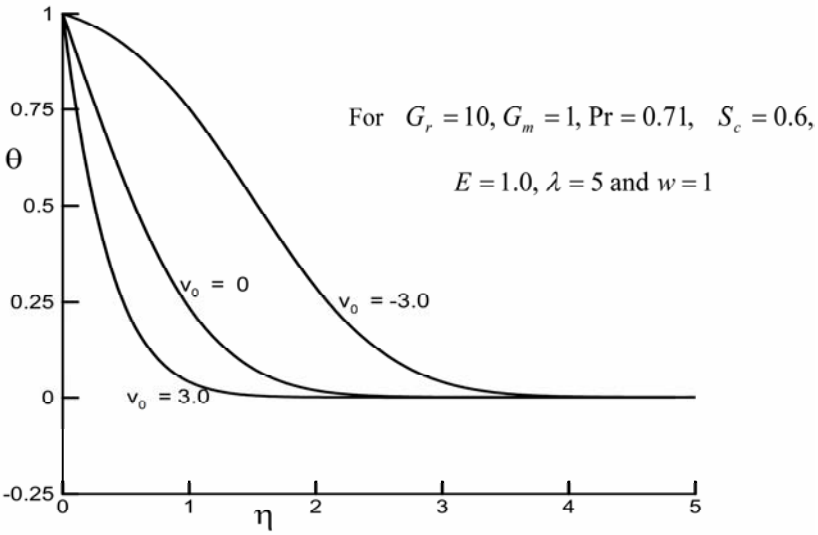

Figure 10. Effects of ν_0 on the temperature profiles.

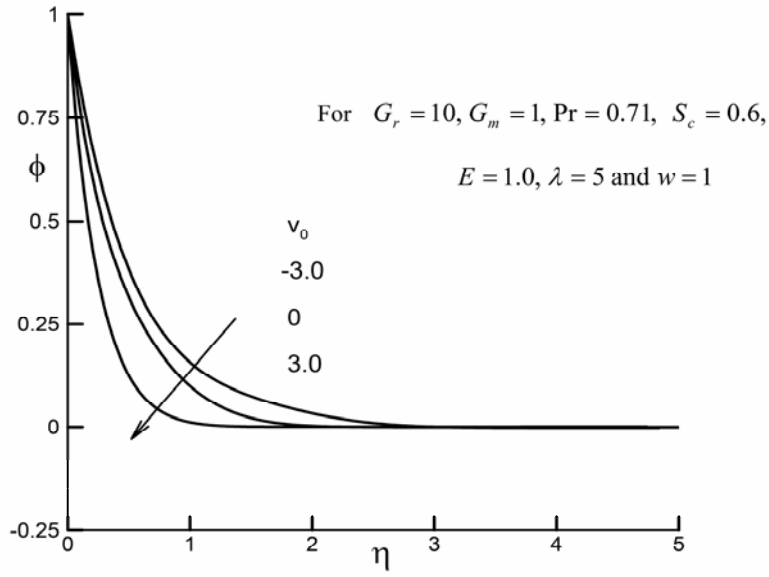

Figure 11. Effects of v_0 on the concentration profiles.

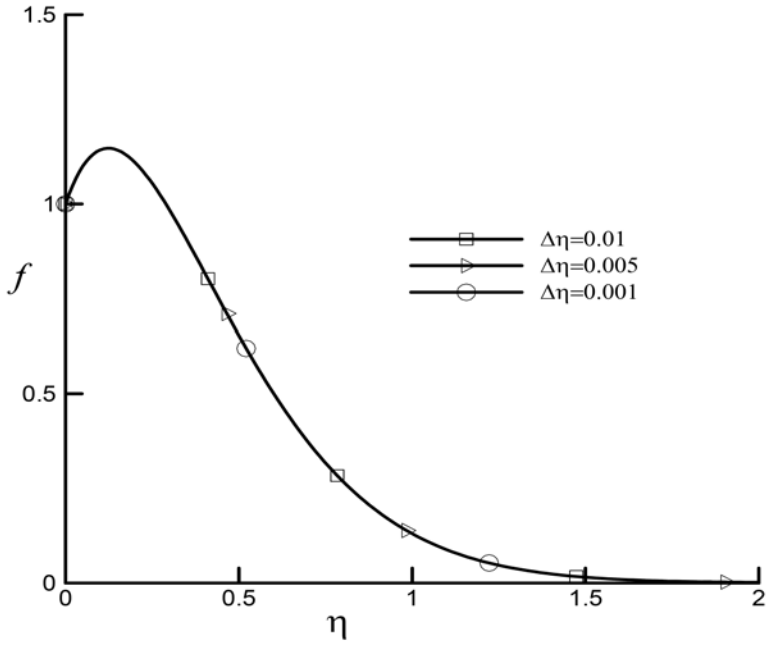

Figure 12. Velocity profiles for different step sizes.

5.5. The skin-friction, the heat transfer, and the mass transfer coefficients

The skin-friction, the heat transfer, and the mass transfer coefficients are tabulated in Table 1 for different values of G_r, λ, E, w, and ν_0. We observe from Table 1 that the skin-friction coefficient $(-f'(0))$ decreases with increase in the Grashof number G_r. It is also observed from Table 1 that the rate of mass transfer coefficient increases with the increasing values of λ and the mass transfer coefficient decreases with the increasing values of E and w. It is observed from this table that, this is an increasing effect of suction parameter ν_0 on the skin friction coefficient, heat and mass transfer coefficients.

Table 1. Effects of G_r, λ, w, E, and ν_0 on the skin friction coefficient, Nusselt number, and the Sherwood number for $G_r = 10$, $G_m = 1$, $P_r = 0.71$, $\nu_0 = 3$, $S_c = 0.6$, $E = 1$, $\lambda = 1$, and $w = 1$

	$-f'(0)$	$-\theta'(0)$	$-\phi'(0)$
$G_r = -10.00000$	6.17604	2.48484	2.33717
-5.00000	4.67836	2.48407	2.33839
0.00000	3.17570	2.48414	2.34003
5.00000	1.67522	2.48493	2.34150
10.00000	0.18154	2.48602	2.34299
$\lambda = 1.00000$	0.23082	2.57692	2.26709
2.00000	0.18154	2.48602	2.34299
3.00000	0.16885	2.37165	2.45143
$w = 0.00000$	0.16179	2.55499	2.29238
0.50000	0.18531	2.56452	2.28638
1.00000	0.23082	2.57692	2.26709
$E = 0.00000$	0.19647	2.48092	2.36456
0.50000	0.22281	2.54820	2.30110
1.00000	0.23510	2.57696	2.28143
2.00000	0.20723	2.59386	2.25421
$\nu_0 = -3.00000$	-3.78943	0.11342	1.59867
0.00000	-3.4529	0.93421	1.85269
3.00000	0.23510	2.57696	2.28143

6. Conclusion

In this paper, we investigate the effects of exothermic chemical reaction rate and Arrhenius activation energy on an unsteady natural convection heat and mass transfer boundary layer flow past a flat porous plate. The Nachtsheim and Swigert [11] iteration technique based on sixth-order Runge-Kutta and shooting method has been employed to complete the integration of the resulting solutions.

The following conclusions can be drawn as a result of the computations:

(1) Velocity increases with increasing values of G_r for the cooling of the plate and the negative increase in the Grashof number leads to the decrease in the velocity field. That is for heating of the plate, the effects of the Grashof number G_r on the velocity field have also opposite effects, as compared to the cooling of the plate.

(2) Solutal Grashof number $G_m > 0$ corresponds that the chemical species concentration in the free stream region is less than the concentration at the boundary surface. It is observed that the velocity profile increases with the increasing values of Solutal Grashof number G_m.

(3) Increase in λ leads to the decrease in the concentration profiles. It is observed from the Equation (1) that increasing temperature frequently causes a marked increase in the rate of reactions λ. The velocity profile slightly increases with the increasing values of λ.

(4) Increase in activation energy (E) leads to increase the concentration, temperature, and velocity profiles.

(5) For strong suction $(\nu_0 > 0)$, the velocity, the temperature, and the concentration profiles decay rapidly away from the surface. As for the injection $(\nu_0 < 0)$, it is observed that the boundary layer is increasingly blown away from the plate to form an interlayer between the injection and the outer flow regions.

References

[1] M. A. Alabraba, A. R. Bestman and A. Ogmu, Laminar convection in binary mixture of hydromagnetic flow with radiative heat transfer, Astrophysics and Space Science 195 (1992), 431-439.

[2] A. Al-Sharif, K. Chamniprasart, K. R. Rajagopal and A. Z. Szeri, Lubrication with binary mixtures: Liquid-liquid emulsion, J. Tribol. 115 (1993), 46-55.

[3] C. E. Beevers and R. E. Craine, On the determination of response function for a binary mixture of incompressible Newtonian fluid, Int. J. Engg. Sci. 20 (1982), 737-745.

[4] A. R. Bestman, Natural convection boundary layerwith and mass transfer in a porous medium, International Journal of Energy Research 14 (1990), 389-396.

[5] A. R. Bestman, Radiative heat transfer to flow of a combustible mixture in a vertical pipe, International Journal of Energy Research 15 (1991), 179-184.

[6] R. Kandasamy, K. Periasami and K. K. Sivagnana Probhu, Effects of chemical reaction, heat and mass transfer along a wedge with heat source and concentration in the presence of suction and injection, International Journal of Heat and Mass Transfer 48 (2005), 1388-1394.

[7] O. D. Makinde, P. O. Olanrewaju and W. M. Charles, Unsteady convection with chemical reaction and radiative heat transfer past a flat porous plate moving through a binary mixture, Africka Matematika AM 21(1) (2011), 1-17.

[8] O. D. Makinde and P. O. Olanrewaju, Unsteady mixed convection with Soret and Dufour effects past a porous plate moving through a binary mixture of chemically reacting fluid, Chemical Engineering Communications 198(7) (2011), 920-938.

[9] Kh. Abdul Maleque, Effects of combined temperature and depth-dependent viscosity and Hall current on an unsteady MHD laminar convective flow due to a rotating disk, Chemical Engineering Communications (Taylor and Francis) 197 (2010), 506-521.

[10] N. Mills, Incompressible mixtures of Newtonian fluids, Int. J. Engg. Sci. 4 (1966), 97-112.

[11] P. R. Nachtsheim and P. Swigert, Satisfaction of asymptotic boundary conditions in numerical solution of system of nonlinear of boundary layer type, NASA TN-D3004, 1965.

[12] Nopparat Pochai and Jiratchaya Jaisaardsuetrong, A numerical treatment of an exothermic reactions model with constant heat source in a porous medium using finite difference method, Advanced Studies in Biology 4(6) (2012), 287-296.

[13] H. Schlichting, Boundary Layer Theory, McGraw Hill Book Co., New York, 1968.

[14] A. K. Singh and C. K. Dikshit, Hydromagnetic flow past a continuously moving semi-infinite plate for large suction, Astrophysics and Space Science 14 (1988), 219-256.

[15] S. Subramanian and V. Balakotaiah, Convective instabilities induced by exothermic reactions occurring in a porous medium, Phys. Fluids 6(9) (1994), 2907-2922.

[16] Michal Tencer, John Seaborn Moss and Trevor Zapach, Arrhenius average temperature: The effective temperature for non-fatigue wearout and long term reliability in variable thermal conditions and climates, IEEE Transactions on Components and Packaging Technologies 27(3) (2004), 602-607.

[17] C. Truesdell, Sulle basi della thermomeccanica, Rend. Lince 22(8) (1957), 33-38; 158-166.

[18] S. R. Wang, A. Al-Sharif, K. R. Rajagopal and A. Z. Szeri, Lubrication with binary mixtures: Liquid-liquid emulsion an EHL conjunction, J. Tribol. 115 (1993), 515-522.

■